**Atmospheric
Measurement
Techniques**

Aerosol Optical Depth measurements at 340 nm with a Brewer spectrophotometer and comparison with Cimel sunphotometer observations at Uccle, Belgium

V. De Bock, H. De Backer, A. Mangold, and A. Delcloo

Royal Meteorological Institute of Belgium, Ringlaan 3, 1180 Brussels, Belgium

Abstract. The Langley Plot Method (LPM) is adapted for the retrieval of Aerosol Optical Depth (AOD) values at 340 nm from Brewer#178 sun scan measurements between 335 and 345 nm (convoluted with the band pass function of the Cimel sunphotometer filter at 340 nm) performed in Uccle, Belgium. The use of sun scans instead of direct sun measurements simplifies the comparison of the AOD values with quasi-simultaneous Cimel sunphotometer values. Also, the irradiance at 340 nm is larger than the one at 320.1 nm due to lower ozone absorption, thus improving the signal to noise ratio. For the selection of the cloudless days (from now on referred to as calibration quality clear days), a new set of criteria is proposed. With the adapted method, individual clear sky AOD values, for which the selection criteria are also presented in this article, are calculated for a period from September 2006 until the end of August 2010. These values are then compared to quasi-simultaneous Cimel sunphotometer measurements, showing a very good agreement (the correlation coefficient, the slope and the intercept of the regression line are respectively 0.974, 0.968 and 0.011), which proves that good quality observations can be obtained from Brewer sun scan measurements at 340 nm. The analysis of the monthly and seasonal Brewer AODs at Uccle is consistent with studies at other sites reporting on the seasonal variation of AODs in Europe. The highest values can be observed in summer and spring, whereas more than 50% of the winter AODs are lower than 0.3. On a monthly scale, the lowest AOD are observed in December and the highest values occur in June and April. No clear weekly cycle is observed for Uccle. The current cloud-screening algorithm is still an issue,

which means that some AOD values can still be influenced by scattered clouds. This effect can be seen when comparing the calculated monthly mean values of the Brewer with the AERONET measurements.

1 Introduction

Aerosols are particles in the solid or liquid phase that are suspended in the atmosphere and have an important influence on the atmospheric chemistry and physics (Cheymol and De Backer, 2003; Raghavendra Kumar et al., 2010). They affect the tropospheric chemical composition, they can reduce visibility and they have important impacts on human health (Unger et al., 2009; Lyamani et al., 2010; Raghavendra Kumar et al., 2010). Aerosols also influence the Earth's radiation budget in a direct, semi-direct and indirect manner. The scattering and absorption of short and long wave radiation is called the direct effect (Ramanathan et al., 2001; Kaufman et al., 2002; Andreae et al., 2005; Myrhe, 2009). The semi-direct effect describes the warming of the boundary layer, through the absorption of radiation by aerosols, which can lead to evaporation of clouds. This will allow more solar radiation to reach the surface (Ramanathan et al., 2001; Cazorla et al., 2009). The indirect effect concerns the ability of aerosols to act as cloud condensation nuclei which influences the microphysical and optical properties of clouds, thus changing the radiative and precipitation properties and the lifetime of clouds (Ramanathan et al., 2001; Kaufman et al., 2002; Lohmann, 2002; Lohmann and Feichter, 2005; Unger et al., 2009). Because of a lack of information concerning the temporal and spatial distribution of aerosols, they are key

Correspondence to: V. De Bock
(veerle.debock@meteo.be)

contributors to the uncertainties in current climate studies (Andreae et al., 2005; IPCC, 2007).

The influence of aerosols on ultraviolet (UV) radiation has received a lot of attention in research, since the impact of UV radiation on human health, the biosphere and atmospheric chemistry strongly depends on the characteristics and quantity of aerosol in the atmosphere. An overexposure to UV-B radiation can lead to serious health damage for humans such as skin cancer, accelerated aging of skin, cataract, photokeratitis (snow blindness) and changes in the immune system (Rieder et al., 2008; Cordero et al., 2009). UV-B radiation also has adverse effects on terrestrial plants (Tevini and Teramura, 1989; Cordero et al., 2009) and on other elements of the biosphere (Diffey, 1991). The increase of anthropogenic aerosols in non-urban areas of the industrialized countries since the industrial revolution is supposed to have decreased the biologically active UV radiation by 5 to 18% (Liu et al., 1991). Accuracy in UV prediction can be improved if the role of aerosols on surface UV radiation is clarified (Kim et al. 2008). However, little information is available on the optical properties of atmospheric aerosols in the UV spectral region, compared to the visible spectral range (Sellitto et al., 2006).

To gain a better understanding of the effect of aerosols in the UV, knowledge of the parameters that determine the optical and physical properties of aerosols is essential (Cazorla et al., 2009; Kazadzis et al., 2009). One of these parameters is the Aerosol Optical Depth (AOD), an integral measurement of the combined aerosol scattering and absorption in the atmospheric column (Mulcahy et al., 2009). When assessing the recovery of the ozone layer, knowledge of the AOD is of high importance. Without such knowledge, it is very likely that a change in surface UV irradiance is attributed to a change in ozone amount, whereas it could actually be the result of an increase or decrease in aerosol load. Several reports have been written on the retrieval of AOD in the UV range. For example, Taylor et al. (2008) and Corr et al. (2009) use MFRSR (Multi Filter Rotating Shadowband Radiometer) measurements for this retrieval. Research also shows that the standard Brewer direct sun (DS) measurements allow AOD retrieval at the wavelengths used for ozone determination (mainly 320.1 nm). Some authors base their retrieval on the absolute calibration of the solar spectral irradiance measured by the Brewer (Bais, 1997; Marenco et al., 1997; Kazadzis et al., 2005) whereas others use the Langley extrapolation method to determine the absolute calibration of the irradiance (Kirchhoff et al., 2001; Marenco et al., 2002; Cheymol and De Backer, 2003). Arola and Koskela (2004) discussed the systematic errors in the AOD retrieval from Brewer DS measurements, which led to improvements of the conventional Langley Plot Method (e.g. Cheymol et al., 2009).

Several authors studied the spatial and temporal patterns in AOD. Both Bäumer et al. (2008) and Xia et al. (2008) reported a weekly cycle in AOD for Central Europe (45–55° N; 0–20° E). Seasonal patterns in AOD with maximum values in spring and summer and minimum values in autumn and winter are observed in many studies (Meleti and Cappellani, 2000; Behnert et al., 2004; Kim et al., 2006; Estellés, 2008; Remer et al., 2008; Che et al., 2009; Léon et al., 2009; Lyamani et al., 2010). Gröbner and Meleti (2004) studied long-term trends in AOD at Ispra and detected a decrease between 1991 and 1997, followed by a stabilization in the AOD values. Kazadzis et al. (2007) however, reported on a statistically significant (99% level) decrease in AOD for Thessaloniki after 1997. Hatzianastassiou et al. (2009) studied the spatial distribution of AOD over the Mediterranean basin and found significant geographical variation of AOD within the study area (e.g. large AOD values over North Africa and smaller values in relatively remote oceanic areas such as Crete island).

In this paper, we present an adapted and improved method for the retrieval of AOD values. Instead of using the standard direct sun measurements from the Brewer instrument dedicated to ozone retrieval (which are performed at 5 specific wavelengths) (as in Cheymol and De Backer, 2003), we will use sun scan measurements between 335 and 345 nm, convoluted with the band pass function of the Cimel sunphotometer filter at 340 nm, to obtain AOD values at 340 nm. This will allow for a direct comparison between these retrieved AOD values and the AODs from the Cimel sunphotometer at the same wavelength. Information about the used instruments and the measurement location is included in Sect. 2. The method applied for the retrieval of the Brewer AOD values is described in Sect. 3. The resulting AOD values are compared with Cimel sunphotometer measurements in Sect. 4. Also, the temporal patterns in AOD are discussed and compared to results of other studies.

2 Instruments and location

In this study, we make use of the measurements of a Brewer spectrophotometer and a Cimel sunphotometer. Both instruments are located in Uccle, a residential suburb of Brussels about 100 km from the shore of the North Sea. The prevailing meteorological conditions will determine whether the station is influenced by sea salt aerosols, by aerosols from urban activity or by continental type of aerosols (De Backer, 2009).

The Brewer spectrophotometer was developed in the early 1980s to measure total ozone in the atmosphere from UV-B radiation (Brewer, 1973; Kerr et al., 1988). The instrument records raw photon counts of the photomultiplier at five wavelengths (306.3, 310.1, 313.5, 316.8 and 320.1 nm) using a blocking slit mask, which opens successively one of the five exit slits. The five exit slits are scanned twice within 1.6 s and this is repeated 20 times. The whole procedure is repeated five times for a total of about three minutes. The total ozone column is obtained from a combination of measurements at 310.1, 313.5, 316.8 and 320.1 nm weighted with a

predefined set of constants chosen to minimize the influence of SO_2 and linearly varying absorption features such as from clouds or aerosols (Gröbner and Meleti, 2004). RMIB (Royal Meteorological Institute of Belgium) has two Brewers on the roof of its building in Uccle ($50°48'$ N, $4°21'$ E, 100 m a.s.l.). Brewer#016 is a single monochromator Mark II model that was installed in Uccle in 1983. In 1989, the instrument was equipped with an automated azimuth and zenith pointing system, resulting in a higher observation frequency (Cheymol et al., 2006). Brewer#178 is a double monochromator Mark III that was installed in September 2001. In addition to the standard observation routines, an additional routine was developed to be able to determine the AOD at 340 nm with the double monochromator Brewer. More precisely, the sun scan routine was adapted to perform scans between 335 nm and 345 nm with slit 1. The measuring wavelength step of this sun scan routine is 0.5 nm and one scan has a duration of 21 s. For comparison with Cimel AOD products, the obtained spectral data are convoluted with the band pass function of the Cimel sunphotometer filter (Full Width at Half Maximum of the filter is 4.756 nm) (standard Cimel sunphotometer filter values; Barr Associates Inc.). The data of this type, available since 17 August 2006, will be used for the retrieval of AOD at 340 nm. The stability of the Brewer#178 wavelengths has been examined and the results show that the stability of this instrument is very good (Gröbner et al. 2006). This justifies the application of the Langley Plot Method (Sect. 3) on the sun scan measurements of Brewer#178 for the retrieval of AOD.

The Cimel sunphotometer, which belongs to BISA (Belgium Institute of Space Aeronomy), is located at approximately 100 m from the Brewer instrument. It is an automatic sun-sky scanning filter radiometer allowing the measurements of the direct solar irradiance at wavelengths 340, 380, 440, 500, 670, 870, 940 and 1020 nm. These solar extinction measurements are used to compute aerosol optical depth at each wavelength except for the 940 nm channel, which is used to retrieve total atmospheric column precipitable water in centimeters. The instrument is part of the AERONET network (http://aeronet.gsfc.nasa.gov/; Holben et al., 2001). The accuracy of the AERONET AOD measurements at 340 nm is 0.02 (Eck et al. 1999).

3 Method

To derive the AOD at 340 nm from the measurements described above, we apply the Langley Plot Method (LPM), in a similar way as described in Cheymol and De Backer (2003), to the weighted irradiances. The Langley Plot Method is a linear regression technique that can be used for the retrieval of the Aerosol Optical Depth from direct radiation measurements. This method can only be applied on cloud-free days and for each cloud-free day, one AOD value and one calibration factor (CF) will be estimated. Due to the

low number of completely cloud-free days, we only applied the LPM once for the entire period. The mean calibration factor (calculated from the individual values for the cloud-free days) will be used to calculate the Aerosol Optical Depth for each individual measurement. The basics of this method and the deviations from the algorithm in Cheymol and De Backer (2003) will be described here. More details on the LPM can be found in Marenco et al. (2002) and in Cheymol and De Backer (2003).

3.1 Basic equation

An important difference between this work and the one by Cheymol and De Backer (2003) is that the latter uses the direct sun (DS) measurements at five specific wavelengths (320.1 nm being the largest) from the Brewer instrument for the received signal values, whereas here we use sun scans between 335 and 345 nm, convoluted with the band pass function of the Cimel sunphotometer filter at 340 nm. The use of the sun scans is an important improvement that simplifies the comparison of the AOD values, since it is no longer necessary to extrapolate the Cimel AOD values to the Brewer wavelength. Moreover, due to the convolution with the Cimel sunphotometer band pass filter, we compare physically exactly the same quantity. Another advantage is that the intensity of the retrieved signal at this wavelength is larger due to the lower absorption by ozone, improving the signal to noise ratio. The signal, received by the Brewer instrument, follows Beer's law (using the notations as in Cheymol and De Backer, 2003):

$$S(\lambda) = K(\lambda)I_0(\lambda)\exp[-\mu\alpha(\lambda,T)\Omega - m\beta(\lambda)\frac{P}{P_{std}}$$
$$-\delta(\lambda)\sec(z_a)], \tag{1}$$

with $S(\lambda)$ the received signal, $K(\lambda)$ the proportionality factor of the instrument's response to the incoming solar radiation at wavelength λ, $I_0(\lambda)$ the irradiance outside the earth's atmosphere at wavelength λ, μ the relative optical air mass (the path length relative to that at the zenith at sea level) of the ozone layer at height=22 km, $\alpha(\lambda,T)$ the ozone absorption coefficient at wavelength λ and temperature T, Ω the equivalent thickness of the ozone layer, m the relative optical air mass of the atmosphere in a thin layer assumed to be at an altitude of 5 km for Rayleigh scattering, $\beta(\lambda)$ the Rayleigh scattering coefficient, P_{std} the standard pressure (1013.25 hPa), P the station pressure (1000 hPa), $\delta(\lambda)$ the aerosol extinction optical thickness of a vertical path through the atmosphere and z_a the zenith angle of the sun.

This law reflects that, while passing through the atmosphere, the direct beam at the top of the atmosphere is subject to absorption and scattering through three different physical phenomena: (a) absorption by ozone, (b) scattering by air molecules (Rayleigh scattering) and (c) extinction by aerosol particles. The SO_2 absorption is not considered here, since this term is very low compared to the ozone absorption

term, which is already small at 340 nm. To eliminate the dependence of the AOD retrieval on the effective ozone temperature, the ozone absorption coefficient is computed using the effective ozone temperature (as in Cheymol and De Backer, 2003). This effective ozone temperature is calculated using ozone and temperature profiles from balloon soundings available at Uccle. Since the sun scans are convoluted with the Cimel sunphotometer band pass filter, we should also convolute the Rayleigh scattering and the ozone absorption coefficients. The convolution was done for the Rayleigh scattering term and this caused only a small change in the retrieved AOD values with a maximum difference of 0.00023 with respect to AOD values calculated without a convoluted Rayleigh term. Since the contribution of the ozone absorption term to the computation of the AOD values is very low compared to the Rayleigh contribution, we did not convolute the ozone absorption coefficient. This would lead to negligible changes in the AOD.

3.2 Langley plot method

Taking the logarithm of Eq. (1) gives Eq. (2):

$$
\ln[S(\lambda)] + \mu\alpha(\lambda)\Omega + m\beta(\lambda)\frac{P}{P_{\text{std}}}
$$
$$
= \ln[K(\lambda)I_0(\lambda)] - \delta(\lambda)\sec(z_{\text{a}}) \tag{2}
$$

Let us define:

$$
Y = \ln[S(\lambda)] + \mu\alpha(\lambda)\Omega + m\beta(\lambda)\frac{P}{P_{\text{std}}}, \tag{3}
$$

$$
\text{CF} = \ln[K(\lambda)I_0(\lambda)], \tag{4}
$$

$$
A = \delta(\lambda), \tag{5}
$$

$$
X = \sec(z_{\text{a}}). \tag{6}
$$

With Eqs. (3–6), Eq. (2) can be simplified to

$$
Y = \text{CF} - A^*X \tag{7}
$$

Now, one AOD value (A) and one calibration factor (CF) can be estimated per day. The quality of the linear regression depends on the range of the solar zenith angles covered during a certain day. Good observations at both high and low solar zenith angles are needed and the atmospheric conditions must remain stable over the day. This leads to different criteria for the selection of the days on which the LPM can be applied (calibration quality clear days). Cheymol et al. (2009) proposed the following criteria:

1. The individual DS data for which the air mass is above 3 are removed.

2. The range of solar zenith angles (SZA) covered by valid DS observations for one day must be at least 20°.

3. The number of individual DS data must be at least 50 per day (i.e. 10 sequences of 5 observations).

4. The ozone column and its standard deviation are computed on each group of 5 individual DS measurements for each wavelength. Data are accepted if the standard deviation is lower than 2.5 DU.

Since in our case sun scans are used instead of DS measurements, these criteria have to be adapted. The test done on the ozone values (4th criterion) loses its significance since the ozone observations of Brewer#178 and the sun scans between 335 nm and 345 nm are not performed simultaneously. Clouds are thus able to influence the irradiance measurements during the sun scan, while the closest ozone observations (in time) could be made under cloudless conditions. Concerning the 2nd criterion, it has to be mentioned that the same SZA range can yield different ranges of air mass for different seasons. Since air mass range is a more important parameter for the quality control of the Langley Plots, the 2nd criterion was changed so that a minimum range limit was placed on the optical air mass instead of on the SZA range. We will retain the upper value of 3 for the air mass (1st criterion), since at higher air masses the irradiances measured by the Brewer become much lower and the instrument becomes much more sensitive to stray light effects. This could thus bias the AOD measurements. The remaining criteria are applied to the sun scans instead of to DS measurements.

Manually verifying whether the selected days are indeed cloudless showed that these criteria were not sufficient. An additional criterion is therefore proposed. It is based on the ratio of the observed and expected irradiance for a certain day. The observed irradiance is obtained from the sun scans between 335 and 345 nm that are convoluted with the band pass function of the Cimel sunphotometer filter. The expected irradiance (under cloudless circumstances) is calculated by the Tropospheric Ultraviolet and Visible Radiation Model (TUV model version 3.0; Madronich, 1993), which uses the band pass function of the Cimel sunphotometer filter at 340 nm. The climatological monthly mean total ozone value and a default constant AOD value (0.7777 as a standard value for polluted air) are used as input parameters for the calculation of the monochromatic radiative transfer. The cloud optical depth and surface albedo are respectively 0 and 0.05. If a certain day is cloudless and the atmospheric conditions are stable, the ratio of the irradiance should be more or less constant throughout the day. For the calculation of the ratio, both the observed and the expected irradiance are normalized to their maximum. (Figure 1 shows the calculated ratios for a cloudless and for a cloudy day.) In this context, a day is considered cloudless if the maximum deviation of the individual ratios (of a day) from the mean ratio is smaller than 20% (different threshold values were tested, but the 20% value generated the best results, meaning that the selected cloudless days were in agreement with the observed cloudless days).
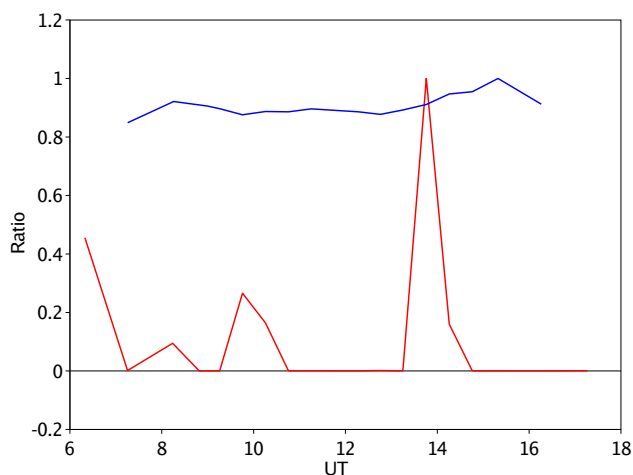
Fig. 1. Ratio of the observed and expected irradiance for a cloudless (5 August 2007; in blue) and for a cloudy (20 July 2008; in red) day at Uccle. The points that appear as null values are points for which the ratio is very small. This can be explained by the influence of clouds, which causes the observed irradiance to be very low.

Table 1. List of selected calibration quality clear days from September 2006 until the end of August 2010 with their calibration factor. The mean calibration factor is calculated from these values.

Date	Calibration Factor
6 Sep 2006	18.485
21 Sep 2006	18.386
4 Apr 2007	18.463
22 Apr 2007	18.527
30 Apr 2007	18.599
1 May 2007	18.434
2 May 2007	18.646
5 May 2008	18.631
8 May 2008	18.593
11 May 2008	18.649
1 Jul 2008	18.568
29 May 2009	18.692
15 Aug 2009	18.584
10 Mar 2010	18.654
23 May 2010	18.638
3 Jun 2010	18.520

This leads to the following set of criteria for the selection of calibration quality clear days (CCD = Criteria Calibration Days) for the determination of the calibration factors with the Langley Plot Method:

1. The sun scans for which the air mass is above 3 are removed.

2. The range of air masses covered by the sun scans for one day must be at least 1.

3. At least 10 sun scans per day have to remain after applying the first two criteria.

4. The maximum deviation of the individual ratios (of the observed and expected irradiance) from the mean ratio for a certain day has to be smaller than 20%.

After applying these criteria, the calibration coefficients are calculated for each selected calibration quality clear day (Table 1). From this calibration coefficient, the mean value is calculated which will be used as mean calibration coefficient of the instrument. With this mean calibration coefficient, the AOD can now be calculated for each individual observation. Since we only apply the Langley Plot Method once for the entire period, the stability of the calibration factor of the instrument can not be calculated. However, the UV-lamp tests of the Brewer instrument, showing that the instrument is very stable, indicate that the same is true for the calibration factor of the instrument. To avoid the influence of clouds that might remain on the calculated AOD values, we only calculated AOD values for the individual sun scans for which a direct sun observation, made with Brewer#178, is available

within a time period of 5 min. It has to be mentioned that this however does not exclude all cloud-perturbed measurements. This is shown in the resulting AOD values, some of which seemed too high to be reliable. As the definition of simple criteria to detect cloud interference in the UV is complex (Dürr and Philipona, 2004) we propose at this stage only a manual method to exclude this cloud contamination. The application of a more sophisticated and automated method will be the subject of a subsequent study. Figure 2 shows the scatter plot of the Brewer AOD measurements and the corresponding Cimel sunphotometer measurements (with a maximum time difference of 30 min). There is a good agreement between Brewer and Cimel for Brewer AOD values lower than 2. When the Brewer AODs become larger than 2, there is virtually no agreement with the Cimel sunphotometer measurements. Based on this result, we decided to automatically remove all Brewer AOD values larger than 2 from our results on the assumption that they were influenced by clouds. No Cimel values were removed, since these values are already cloud-screened.

A set of criteria to select the individual clear sky AOD values (from all the calculated AOD values), can now be defined (CICA = Criteria Individual Clear sky AOD):

1. A direct sun observation must be available for each individual AOD measurement within a time period of 5 min.

2. Each individual AOD value must be lower than 2. Larger values are removed from the results.

The remaining Brewer AOD values were compared to quasi-simultaneous Cimel AODs at 340 nm (AERONET level 2.0 data). Only quasi-simultaneous measurements of
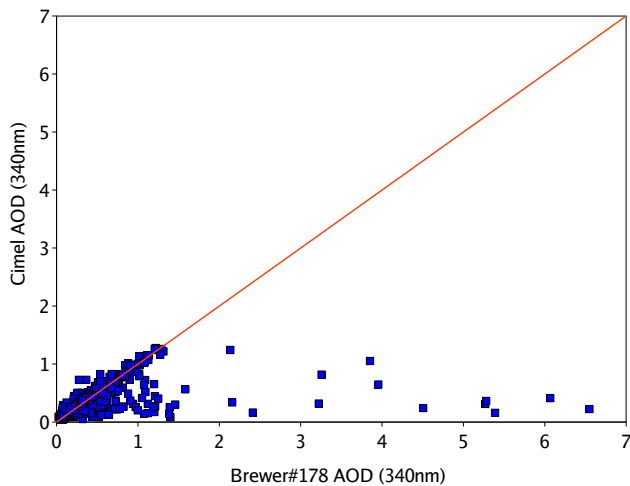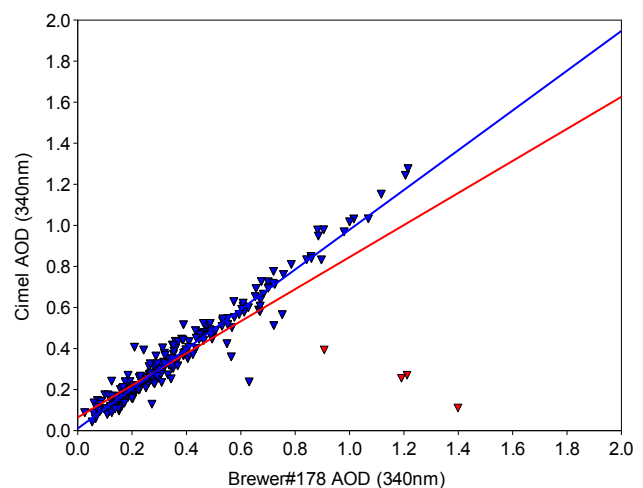
Fig. 2. Scatter plot of the Brewer and Cimel AOD at 340 nm (time period for the comparison is 30 min). The red curve represents $f(x) = x$.

Fig. 3. Comparison of the Brewer and Cimel AOD values at 340 nm (time period for the comparison is 3 min). The red curve ($f(x) = 0.781x + 0.065$) represents the regression line of all the data. The blue curve ($f(x) = 0.968x + 0.011$) shows the regression line of the data without the outliers.

both instruments (with a maximum time difference of 3 min) are considered. The AOD values from Brewer#178 at 320 nm were also compared to quasi-simultaneous Cimel values. A second order fit of ln(AOD) to ln(λ) (using the AERONET data from 500, 440, 380 and 340 nm) was used to estimate the Cimel AOD values at 320 nm.

4 Results and discussion

4.1 Comparison between Brewer spectrophotometer and Cimel sunphotometer measurements

For the comparison with the AOD values from the Cimel sunphotometer, the Brewer#178 sun scan measurements at 340 nm from September 2006 until the end of August 2010 were used. For this period, a total of 16 calibration quality clear days (Table 1) were selected using CCD (as mentioned in Sect. 3.2) combined with individual inspection. The mean calibration factor (CF) for these days is 18.567 ± 0.089. With this calibration coefficient, the individual clear sky AOD values (according to CICA) are calculated, using the Brewer#178 sun scans. The applied method resulted in 2951 AODs at 340 nm for a period from 1 September 2006 to 31 August 2010. The uncertainty in the calibration coefficient (0.089) causes an uncertainty of 0.08 in the AOD measurements. Only quasi-simultaneous measurements from the Brewer and Cimel (level 2.0 data from AERONET) were used for comparison. From the 2951 individual Brewer AODs, only 251 measurements had a quasi-simultaneous Cimel measurement. The comparison of the Brewer and Cimel AODs at 340 nm had a correlation coefficient of 0.860 (Fig. 3). Selecting only those Brewer AOD observations with a concurrent Cimel sunphotometer observation (maximum

time difference of 3 min) and with a quasi-simultaneous DS measurement (maximum time difference of 5 min) automatically eliminates most of the cloudy conditions. The scatter plot of the compared AODs still showed the presence of a few outliers (highlighted in red in Fig. 3), causing the rather low correlation coefficient compared to the one obtained by Cheymol et al. (2009) (correlation coefficient of 0.96 for the comparison between Brewer#016 at 320 nm and Cimel at 340 nm). These remarkable outliers require further examination. We consider a single point in the scatter plot to be an outlier if the difference in AOD between Brewer and Cimel measurements is bigger than 0.5. This is the case for less than 2% of the compared values which made us question those individual Brewer measurements for which the difference was higher than 0.5. All the sun scan measurements of days with an outlier were plotted. Figure 4 shows the theoretical and the observed relative intensity of the irradiance for a day on which an outlier was present (13 September 2006). The figure clearly shows that the outlier measurement (highlighted in red) is influenced by clouds. This justifies the removal of this point from the comparison. Similar checks were performed for the other outliers and it turned out that for those outliers, the Brewer measurements were made under cloud-perturbed circumstances. Then a comparison was made excluding these outliers. This resulted in a much higher correlation coefficient of 0.974. The slope is 0.968 ± 0.014 and the intercept is 0.011 ± 0.006 (Fig. 3), confirming a good linear agreement between the AOD measurements of both instruments. The agreement between the AODs at 340 nm is better than at 320 nm (Fig. 5), where the correlation is 0.900, the slope 0.863 ± 0.021 and the intercept 0.025 ± 0.010. This shows that good quality AOD
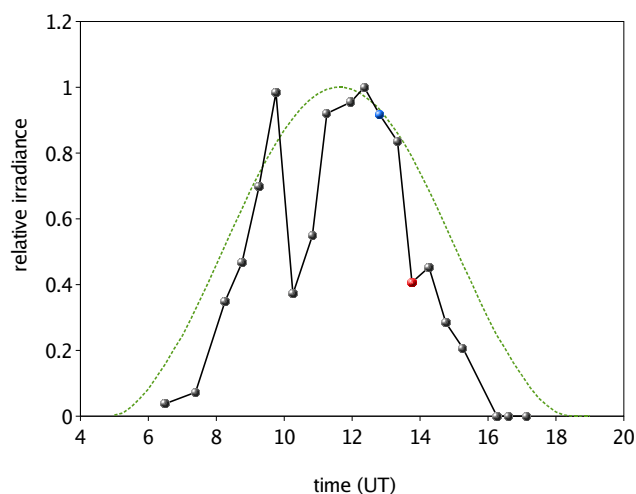
Fig. 4. Sun scan measurements of Brewer#178 on a day for which an outlier was present (13 September 2006). The green dashed line represents the theoretical values, based on the output of the TUV model, whereas the black line represents the observed relative intensity of the irradiance. The highlighted points (red and blue) represent the points for which the comparison with the Cimel measurements was done (which means there was a Cimel observation within a time period of 3 min). The difference between the Brewer and Cimel measurements was larger than 0.5 for the red point, which was considered to be an outlier. From this plot, it is clear that this outlier measurement is strongly influenced by clouds.

observations can be obtained at 340 nm from Brewer#178 sun scan measurements with the proposed method. A comparison is also made between the monthly mean AOD values (Fig. 7) from the Brewer and Cimel measurements. For some months, the difference between the monthly values is rather high. For example in March 2008, the mean monthly Cimel AOD was 0.16, whereas for the Brewer instrument, the monthly mean was 0.54. For 13 months (out of the analyzed 27 months) the difference between the monthly AOD values of the two instruments is larger than 0.2. The mean monthly AOD values of the Brewer instrument are most likely upper limits, since some individual AOD measurements (that constitute to these values) can still be highly biased as a result of cloud perturbation. This thus causes the large differences in mean monthly values between the two instruments. It also shows that the used cloud-screening method needs further improvement.

4.2 AOD variability in Uccle on different timescales

A total of 2951 individual AOD measurements from Brewer#178 were calculated for the period from 1 September 2006 to 31 August 2010 and the values were examined for possible variations on seasonal, monthly and weekly timescales. Some of the individual AOD values were questionable, especially the values larger than 1.5. When Brewer and Cimel measurements were compared, these values were
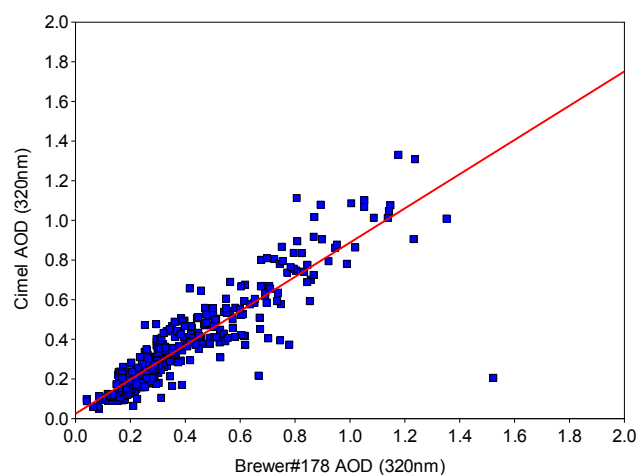

Fig. 5. Comparison of the Brewer#178 and Cimel AOD values at 320 nm. The red line is the linear regression curve ($f(x) = 0.863x + 0.025$) of the comparison.

automatically removed from the results because the Brewer AOD values larger than 1.5 did not have a concurrent Cimel measurement. However, for the study of the individual values in the whole archive (which are not compared to the Cimel data) it is required to manually check the data for cloud-perturbed measurements. For each day with an AOD measurement higher than 1.5, a plot was made of the measured irradiances (photon counts) from the Brewer instruments. If the relative irradiance is much lower than one would expect, the measurement is perturbed (by clouds) and the individual AOD value will thus be removed from the results. So, next to the automatic cloud-screening (using CICA), a manual check is done for the individual AOD values larger than 1.5. An objective method to remove observations affected by clouds is under development. The outlier values from the comparison with the Cimel are also not included in the analyzed dataset. The remaining 2834 individual AOD values were used to study variability on different time scales.

4.2.1 Seasonal and monthly variability

Many studies that investigate the seasonal variability of aerosols, report high AODs during summer (June, July, August) and spring (March, April, May) and low AODs in winter (December, January, February) and autumn (September, October, November). In Valencia (Spain), maximum AOD values were observed (between 2002–2005) from June to September, whereas the minimum values occurred from October to February (mainly in December and January) (Estellés, 2008). Behnert et al. (2004) observed two peak periods in the AOD values from Helgoland Island, Hamburg, Oostende and Lille. They occurred during spring (April–May) and summer (July–August). Studies in Ispra (Italy),
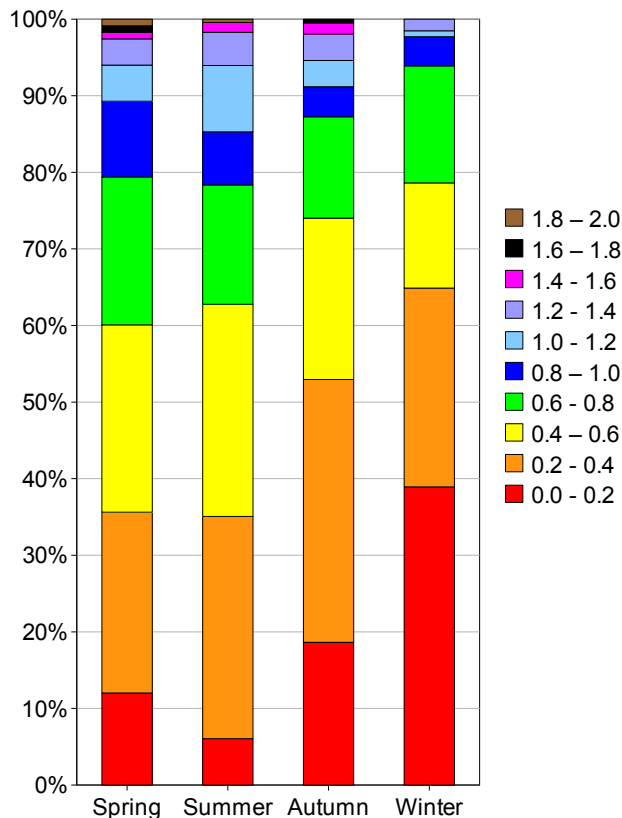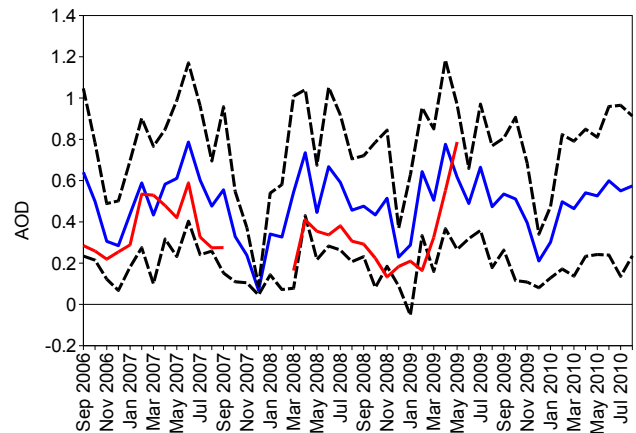
Fig. 6. Seasonal frequency distribution of AOD values at 340 nm at Uccle from 1 September 2006 to 31 August 2010.


Fig. 7. Monthly variation in AOD (at 340 nm) at Uccle (based on data from September 2006 until the end of August 2010). The blue line is the mean seasonal value, whereas the dashed black lines represent the mean value ± its standard deviation. For December 2007, the mean monthly value is based on only 3 individual AOD values (which were accidentally very close). This explains the low standard deviation for this month. The AERONET level 2.0 monthly means are shown in red.

Table 2. List of places mentioned in this article with their latitude and longitude.

Location	Latitude	Longitude
Uccle (Belgium)	50°48′ N	4°21′ E
Oostende (Belgium)	51°13′ N	2°55′ E
Lille (France)	50°36′ N	3°06′ E
Helgoland Island (Germany)	54°10′ N	7°53′ E
Hamburg (Germany)	53°34′ N	9°56′ E
Ispra (Italy)	45°49′ N	8°38′ E
Valencia (Spain)	39°30′ N	0°25′ W
Granada (Spain)	37°10′ N	35°35′ E
Thessaloniki (Greece)	40°30′ N	22°54′ E
Beijing (China)	39°59′ N	116°19′ E
Gwangju (Korea)	35°13′ N	126°50′ E
M'Bour (Senegal)	16°58′ N	14°23′ E

Granada (Spain), M'Bour (Senegal), Gwangju (Korea) and Thessaloniki (Greece) also show high AOD values in summer and low values in winter (Meleti and Cappellani, 2000; Kim et al., 2006; Kazadzis et al., 2007; Léon et al., 2009; Lyamani et al., 2010). (The latitude and longitude of the places mentioned in this article can be found in Table 2.)

The obtained AODs from Brewer#178 at Uccle are consistent with these studies. Figures 6 and 7 display the seasonal and monthly variation in AOD values for Uccle. The highest values can be observed in summer (respectively 0.63(±0.35), 0.59(±0.34), 0.53(±0.27) and 0.58(±0.37) for 2007, 2008, 2009 and 2010) and spring (respectively 0.55(±0.32), 0.58(±0.35), 0.63(±0.38) and 0.51(±0.30) for 2007, 2008, 2009 and 2010). In winter more than 50% of the AODs at Uccle are below 0.3, which is in agreement with the results from Kazadzis et al. (2007) for Thessaloniki, Greece. On a monthly scale (Fig. 7), the lowest AODs are observed in December (respectively 0.07(±0.02), 0.23(±0.14) and 0.21(±0.13) for 2007, 2008 and 2009), whereas the highest values occur in June (0.79(±0.38)) in 2007 and April (0.74(±0.31) in 2008 and 0.78(±0.41) in 2009).

Possible explanations for the higher summer AODs are given by several authors. Behnert et al. (2004) attribute the summer peak values to the slowing down of air mass circulation in summer and the production of smog. This results in an accumulation of high aerosol concentrations above midlatitude regions. Kaskaoutis et al. (2007) explain the higher summer AODs at Ispra as a result of the absence of wet removal processes. According to Kazadzis et al. (2007), the enhanced evaporation and the higher temperatures during summer in Thessaloniki cause a rise in the turbidity of the boundary layer. Combined with stagnating weather systems, this will lead to the formation of aerosols. In winter, there is a significant amount of wet deposition of aerosols, which will cause a cleaning of the atmosphere and therefore lower AOD values. Koelemeijer et al. (2006) also state that
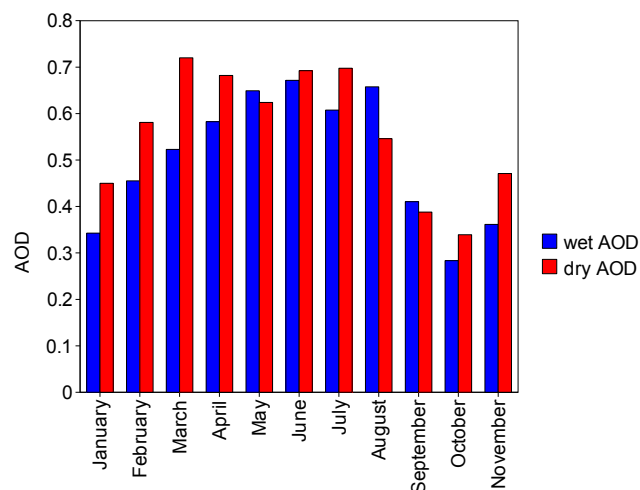
Fig. 8. Mean monthly AOD values (at 320 nm from Brewer#016) for dry and wet days for a time period from 1984 to 2009.

Table 3. Mean AOD values at 340 nm and their standard deviations for each day of the week.

Day of the week	Mean AOD
Monday	0.49 ± 0.29
Tuesday	0.50 ± 0.34
Wednesday	0.53 ± 0.32
Thursday	0.51 ± 0.35
Friday	0.52 ± 0.30
Saturday	0.52 ± 0.36
Sunday	0.50 ± 0.37

high precipitation in winter leads to low AOD values. They observed an anti-correlation (-0.41 for the region of Belgium and The Netherlands) between precipitation and mean monthly AOD. We calculated a correlation of -0.24 between the mean monthly AOD and the monthly percentage of rain days at Uccle for a period between 1984 and 2009. The used AOD values are calculated from Brewer#016 observations at 320 nm, since our time series from Brewer#178 at 340 nm is too short. In order to get a better view of the possible relationship between AOD and precipitation, we divided the calculated AOD values from 1984 to 2009 in two categories, "dry AODs" and "wet AODs", based on the influence of precipitation on the values. We considered a single AOD value to be wet if precipitation was observed on this day or on the previous day. If both days were precipitation-free, we considered the AOD value to be representative for a dry day. Figure 8 shows the mean monthly AOD for the dry and for the wet days. It can be seen that during late autumn, winter and early spring (November–April) the dry AODs are clearly higher than the wet values. The difference is less obvious for the late spring, summer and early autumn months. This could be due to the rather frequent occurrence of local thunderstorms in these seasons, causing only local deposition of aerosols. Air flowing from other places can transport aerosol masses that were not influenced by these local thunderstorms and the measured AOD can thus be higher than one would expect based on the precipitation associated with the thunderstorms. In winter, precipitation is mainly related to the passage of large frontal systems. The wet deposition of the aerosols will thus be spread over a larger region. According to Cheymol and De Backer (2003), a relation with a pollution cycle or with a general circulation could be an explanation of the annual cycle in AOD at Uccle. The seasonal variation of the mixing layer height, which is smaller

in winter and autumn, could be another explanation for the lower AOD in winter and autumn compared to summer and spring where the mixing layer height is thicker. The correlation between the monthly mean mixing layer height and the monthly mean AOD is 0.701 for Uccle. The correlation decreased strongly when the daily mean mixing layer height and the daily mean AOD are compared (correlation of 0.196).

4.2.2 Weekly periodicity

Bäumer et al. (2008) and Xia et al. (2008) observed a weekly AOD cycle in Central Europe. They recorded the lowest values on Sunday and Monday, whereas higher values occurred between Wednesday and Saturday. This cycle is greater for the urban sites than for the rural sites. For our measurements in Uccle, there is no clear signal for such a weekly cycle (Table 3). The largest difference in mean AOD value occurs between Monday and Wednesday (respectively 0.49 versus 0.53). Because of the rather high standard deviation on the average values, we can not state that this difference is a clear signal of a weekly cycle.

5 Summary and conclusions

Aerosols are the most important source of uncertainty in current climate change research (IPCC, 2007). Therefore knowledge of optical and physical properties of aerosols, such as the Aerosol Optical Depth, is essential to gain a better understanding in their effects. In this perspective, an adapted method was developed to retrieve AOD values at 340 nm from Brewer#178 sun scan measurements at Uccle, which allowed for a direct comparison with AOD values from the co-located Cimel sunphotometer at the same wavelength. The retrieval of the Brewer AOD values was based on the Langley Plot Method (as described in Cheymol and De Backer, 2003). For this linear regression technique, the calibration quality clear days in the time period for which the AOD is to be calculated, have to be selected. The criteria from Cheymol et al. (2009) had to be adapted so that they could be applied on sun scan measurements instead of

direct sun measurements. Also, a new criterion, based on the ratio of the observed and expected irradiance for a certain day, was added since the adapted criteria were not sufficient. This led to a new set of criteria for the selection of the calibration quality clear days (CCD). The selected days were then used to determine the mean calibration coefficient of the instrument. With this coefficient, the individual clear sky AOD values (selected using CICA) were calculated from the Brewer sun scans. These values were then compared to the AOD values from the Cimel sunphotometer. After removing the outliers from the comparison, the correlation between the Brewer#178 and Cimel measurements was 0.974, the slope was 0.968 ± 0.014 and the intercept was 0.011 ± 0.006. This proves that there is a very good linear agreement between the AOD measured by both instruments and that good quality AOD observations can be obtained at 340 nm from the sun scans of Brewer#178. The seasonal and monthly variability of the Brewer AODs is consistent with other studies that report on higher AOD values during spring and summer and lower values in autumn and winter. No clear weekly cycle is present for the measurements in Uccle.

Still some AOD measurements perturbed by clouds may exist, which are not removed by the automatic and manual cloud-screening. Currently, the automatic cloud-screening selects the sun scan measurements that have a direct sun measurement within a time period of 5 min for the calculation of the AOD. The individual AOD measurements larger than 2 are automatically removed from the results, since these values are very unlikely for our location. During the manual screening, AOD values larger than 1.5 are removed when the scatter plot of the measured irradiance (i.e. photon counts) shows that the AODs are calculated under cloudy circumstances. The influence of scattered clouds on our measurements is still an issue for the calculation of the AOD values and the current cloud-screening algorithm has to be improved to further increase the quality and reliability of the data.

Edited by: O. Torres

References

Andreae, M. O., Jones, C. D. and Fox, P. M.: Strong present-day aerosol cooling implies a hot future, Nature, 435, 1187–1190, doi:10.1038/nature03671, 2005.

Arola, A. and Koskela, T.: On the sources of bias in aerosol optical depth retrieval in the UV range, J. Geophys. Res., 109, D08209, doi:10.1029/2003JD004375, 2004.

Bais, A. F.: Absolute spectral measurements of direct solar ultraviolet irradiance with a brewer spectrophotometer, Appl. Optics, 36(21), 5199–5204, doi:10.1364/AO.36.005199, 1997

Bäumer, D., Rinke, R., and Vogel, B.: Weekly periodicities of Aerosol Optical Thickness over Central Europe – evidence of an anthropogenic direct aerosol effect, Atmos. Chem. Phys., 8, 83–90, doi:10.5194/acp-8-83-2008, 2008.

Behnert, I., Matthias, V., and Doerffer, R.: Aerosol optical thickness and its spectral dependence derived from sun photometer measurements over the southern North Sea coastal region, Óptica pura y aplicada, 37(3), 3253–3257, 2004.

Brewer, A. W.: A replacement for the Dobson spectrophotometer, Pure Appl. Geophys., 106–108, 919–927, doi:10.1007/BF00881042, 1973.

Cazorla, A., Shields, J. E., Karr, M. E., Olmo, F. J., Burden, A., and Alados-Arboledas, L.: Technical Note: Determination of aerosol optical properties by a calibrated sky imager, Atmos. Chem. Phys., 9, 6417–6427, doi:10.5194/acp-9-6417-2009, 2009.

Che, H., Zhang, X., Chen, H., Damiri, B., Goloub, P., Li, Z., Zhang, X., Wei, Y., Zhou, H., Dong, F., Li, D., and Zhou, T.: Instrument calibration and aerosol optical depth validation of the Chinese Aerosol Remote Sensing Network, J. Geophys. Res., 114, D03206, doi:10.1029/2008JD011030, 2009.

Cheymol, A. and De Backer, H.: Retrieval of the aerosol optical depth in the UV-B from Brewer ozone measurements over a long time period 1984–2002, J. Geophys. Res., 108(D24), 4800, doi:10.1029/2003JD003758, 2003.

Cheymol, A., De Backer, H., Josefsson, W., and Stübi, R.: Comparison and validation of the aerosol optical depth obtained with the Langley plot method in the UV-B from Brewer Ozone Spectrophotometer measurements, J. Geophys. Res., 111, D16202, doi:10.1029/2006JD007131, 2006.

Cheymol, A., Gonzalez Sotelino, L., Lam, K. S., Kim, J., Fioletov, V., Siani, A. M., and De Backer, H.: Intercomparison of Aerosol Optical Depth from Brewer Ozone spectrophotometers and CIMEL sunphotometers measurements, Atmos. Chem. Phys., 9, 733–741, doi:10.5194/acp-9-733-2009, 2009.

Cordero, R. R., Seckmeyer, G., Pissulla, D., and Labbe, F.: Exploitation of spectral direct UV irradiance measurements, Metrologia, 46, 19–25, doi:10.1088/0026-1394/46/1/003, 2009.

Corr, C. A., Krotkov, N., Madronich, S., Slusser, J. R., Holben, B., Gao, W., Flynn, J., Lefer, B., and Kreidenweis, S. M.: Retrieval of aerosol single scattering albedo at ultraviolet wavelengths at the T1 site during MILAGRO, Atmos. Chem. Phys., 9, 5813–5827, doi:10.5194/acp-9-5813-2009, 2009.

De Backer, H.: Time series of daily erythemal UV doses at Uccle, Belgium, Int. J. Remote Sens., 30(15), 4145–4145, doi:10.1080/01431160902825032, 2009.

Diffey, B. L.: Solar ultraviolet radiation effects on biological systems, Phys. Med. Biol., 36(3), 299–328, doi:10.1088/0031-9155/36/3/001, 1991.

Dürr, B. and Philipona, R.: Automatic cloud amount detection by

surface longwave downward radiation measurements, J. Geophys. Res., 109, D05201, doi:10.1029/2003JD004182, 2004.

Eck, T. F., Holben, B. N., Reid, J. S., Dubovik, O., Smirnov, A., O'Neill, N. T., Slutsker, I., and Kinne, S.: Wavelength dependence of the optical depth of biomass burning, urban, and desert dust aerosols, J. Geophys. Res., 104(D24), 31333–31349, doi:10.1029/1999JD900923, 1999.

Estellés, V., Martinez-Lozano, J. A., Utrillas, M. P., and Campanelli, M.: Columnar aerosol properties in Valencia (Spain) by ground-based Sun photometry, J. Geophys. Res., 112, D11201, doi:10.1029/2006JD008167, 2008.

Gröbner, J. and Meleti, C.: Aerosol optical depth in the UVB and visible wavelength range from Brewer spectrophotometer direct irradiance measurements: 1991–2002, J. Geophys. Res., 109, D09202, doi:10.1029/2003JD004409, 2004.

Gröbner, J., Blumthaler, M., Kazadzis, S., Bais, A., Webb, A., Schreder, J., Seckmeyer, G., and Rembges, D.: Quality assurance of spectral solar UV measurements: results from 25 UV monitoring sites in Europe, 2002 to 2004, Metrologia, 43, S66, doi:10.1088/0026-1394/43/2/S14, 2006.

Hatzianastassiou, N., Ghikas, A., Mihalopoulos, N., Torres, O., and Katsoulis, B. D.: Natural versus anthropogenic aerosols in the eastern Mediterranean basin derived from multiyear TOMS and MODIS satellite data, J. Geophys. Res., 114, D24202, doi:10.1029/2009JD011982, 2009.

Holben, B. N., Tanré, D., Smirnov, A., Eck, T. F., Slutsker, I., Abuhassan, N., Newcomb, W. W., Schafer, J. S., Chatenet, B., Lavenu, F., Kaufman, Y. J., Vande Castle, J., Setzer, A., Markham, B., Clark, D., Frouin, R., Halthore, R., Karneli, A., O'Neill, N. T., Pietras, C., Pinker, R. T., Voss, K., and Zibordi, G.: An emerging ground-based aerosol climatology: Aerosol optical depth from AERONET, J. Geophys. Res., 106(D11), 12067–12097, doi:10.1029/2001JD900014, 2001.

Intergovernmental Panel on Climate Change 2007: The physical science, Technical summary of the working group I report, Cambridge University Press, New York, 2007.

Kaskaoutis, D. G., Kambezidis, H. D., Hatzianastassiou, N., Kosmopoulos, P. G., and Badarinath, K. V. S.: Aerosol climatology: on the discrimination of aerosol types over four AERONET sites, Atmos. Chem. Phys. Discuss., 7, 6357–6411, doi:10.5194/acpd-7-6357-2007, 2007.

Kaufman, Y. J., Tanré, D., and Boucher, O.: A satellite view of aerosols in the climate system, Nature, 419, 215–223, doi:10.1038/nature01091, 2002.

Kazadzis, S., Bias, A., Kouremeti, N., Geraspoulos, E., Garane, K., Blumthaler, M., Schallhart, B., and Cede, A.: Direct spectral measurements with a Brewer spectroradiometer: absolute calibration and aerosol optical depth retrieval, Appl. Optics, 44(9), 1681–1690, doi:10.1364/AO.44.001681, 2005.

Kazadzis, S., Bais, A., Amiridis, V., Balis, D., Meleti, C., Kouremeti, N., Zerefos, C. S., Rapsomanikis, S., Petrakakis, M., Kelesis, A., Tzoumaka, P., and Kelektsoglou, K.: Nine years of UV aerosol optical depth measurements at Thessaloniki, Greece, Atmos. Chem. Phys., 7, 2091–2101, doi:10.5194/acp-7-2091-2007, 2007.

Kazadzis, S., Kouremeti, N., Bais, A., Kazantzidis, A., and Meleti, C.: Aerosol forcing efficiency in the UVA region from spectral solar irradiance measurements at an urban environment, Ann. Geophys., 27, 2515–2522, doi:10.5194/angeo-27-2515-2009, 2009.

Kerr, J. B., Asbridge, I. A., and Evans, W. F. J.: Intercomparison of total ozone measured by the Brewer and Dobson spectrophotometer at Toronto, J. Geophys. Res., 93(D9), 11129–11140, doi:10.1029/JD093iD09p11129, 1988.

Kim, J. E., Kim, Y. J., and He, Z.: Temporal variation and measurement uncertainty of UV aerosol optical depth measured from April 2002 to July 2004 at Gwangju, Korea, Atmos. Res., 81, 111–123, doi:10.1016/j.atmosres.2005.11.006, 2006.

Kim, J. E., Ryu, S. Y., and Kim, Y. J.: Determination of radiation amplification factor of atmospheric aerosol from the surface UV irradiance measurement at Gwangju, Korea, Theor. Appl. Climatol., 91, 217–228, doi:10.1007/s00704-006-0285-x, 2008.

Kirchhoff, V. W. J. H., Silva, A. A., Costa, C. A., Paes Leme, N., Pavão, H. G., and Zaratti, F.: UV-B optical thickness observations of the atmosphere, J. Geophys. Res., 106(D3), 2963–2973, doi:10.1029/2000JD900506, 2001.

Koelemeijer, R. B. A., Homan, C. D., and Matthijsen, J.: Comparison of spatial and temporal variations of aerosol optical thickness and particulate matter over Europe, Atmos. Environ., 40, 5304–5315, doi:10.1016/j.atmosenv.2006.04.044, 2006.

Léon, J.-F., Derimian, Y., Chiapello, I., Tanré, D., Podvin, T., Chatenet, B., Diallo, A., and Deroo, C.: Aerosol vertical distribution and optical properties over M'Bour (16.96° W; 14.39° N), Senegal from 2006 to 2008, Atmos. Chem. Phys., 9, 9249–9261, doi:10.5194/acp-9-9249-2009, 2009.

Liu, S. C., McKeen S. A., and Madronich, S.: Effect of anthropogenic aerosols on biologically active ultraviolet radiation, Geophys. Res. Lett., 18(12), 2265–2268, doi:10.1029/91GL02773, 1991.

Lohmann, U.: Possible aerosol effects on ice clouds via contact nucleation, J. Atmos. Sci., 59(3), 647–656, 2002.

Lohmann, U. and Feichter, J.: Global indirect aerosol effects: a review, Atmos. Chem. Phys., 5, 715–737, doi:10.5194/acp-5-715-2005, 2005.

Lyamani, H., Olmo, F. J., and Alados-Arboledas, L.: Physical and optical properties of aerosols over an urban location in Spain: seasonal and diurnal variability, Atmos. Chem. Phys., 10, 239–254, doi:10.5194/acp-10-239-2010, 2010.

Madronich, S.: UV radiation in the natural and perturbed atmosphere, in: Teveni, M. (Ed.), Environmental Effects of Ultraviolet Radiation, Lewis, Boca Raton, FL., 17–69, 1993.

Marenco, F., di Sarra, A., and Di Luisi, J.: Methodology for determining aerosol optical depth from Brewer 300-320nm ozone measurements, Appl. Optics, 41(9), 1805–1814, doi:10.1364/AO.41.001805, 2002.

Marenco, F., Santacesaria, V., Bais, A. F., Balis, D., di Sarra, A., Papayannis, A., and Zerefos, C.: Optical properties of tropospheric aerosols determined by lidar and spectrophotometric measurements (Photochemical Activity and Solar Ultraviolet Radiation campaign), Appl. Optics, 36(27), 6875–6886, doi:10.1364/AO.36.006875, 1997.

Meleti, C. and Cappellani, F.: Measurements of aerosol optical depth at Ispra: Analysis of the correlation with UV-B, UV-A and total solar irradiance, J. Geophys. Res., 105(D4), 4971–4978, doi:10.1029/1999JD900459, 2000.

Mulcahy, J. P., O'Dowd, C. D. and Jennings, S. G.: Aerosol optical depth in clean marine and continental northeast Atlantic air, J. Geophys. Res., 114, D20204, doi:10.1029/2009JD011992, 2009.

Myrhe, G.: Consistency between satellite derived and modelled estimates of the direct aerosol effect, Science, 325(187), 187–190, doi:10.1126/science.1174461, 2009.

Raghavendra Kumar, K., Narasimhulu, K., Balakrishnaiah, G., Suresh Kumar Reddy, B., Rama Gopal, K., Reddy, R. R., Satheesh, S. K., Krishna Moorthy, K., and Suresh Babu, S.: A study on the variations of optical and physical properties of aerosols over a tropical semi-arid station during grassland fire, Atmos. Res., 95, 77–87, doi:10.1016/j.atmosres.2009.08.012, 2010.

Ramanathan, V., Crutzen, P. J., Kiehl, J. T., and Rosenfeld, D.: Aerosols, climate and the hydrological cycle, Science, 294, 2119–2121, doi:10.1126/science.1064034, 2001.

Remer, L., Kleidmann, R. G., Levy, R. C., Kaufman, Y. J., Tanré, D., Mattoo, S., Vanderlei Martins, J., Ichoku, C., Koren, I., Yu, H., and Holben, B. N.: Global aerosol climatology from the MODIS satellite sensors, J. Geophys. Res., 113, D14S07, doi:10.1029/2007JD009661, 2008.

Rieder, H. E., Holawe, F., Simic, S., Blumthaler, M., Krzyscin, J. W., Wagner, J. E., Schmalwieser, A. W., and Weihs, P.: Reconstruction of erythemal UV-doses for two stations in Austria: a comparison between alpine and urban regions, Atmos. Chem. Phys., 8, 6309–6323, doi:10.5194/acp-8-6309-2008, 2008.

Sellitto, P., di Sarra, A., and Siani, A. M.: An improved algorithm for the determination of aerosol optical depth in the ultraviolet spectral range from Brewer spectrophotometer observations, J. Opt. A – Pure Appl. Op., 8, 849–855, doi:10.1088/1464-4258/8/10/005, 2006.

Taylor, T. E., L'Ecuyer, T. S., Slusser, J. R., Stephens, G. L., and Goering, C. D.: An operational retrieval algorithm for determining aerosol optical properties in the ultraviolet, J. Geophys. Res., 113, D03201, doi:10.1029/2007JD008661, 2008.

Tevini, M. and Teramura, H. A.: UV-B effects on terrestrial plants, Photochem. Photobiol., 50, 479–487, doi:10.1111/j.1751-1097.1989.tb05552.x, 1989

Unger, N., Menon, S., Koch, D. M., and Shindell, D. T.: Impacts of aerosol-cloud interactions on past and future changes in tropospheric composition, Atmos. Chem. Phys., 9, 4115–4129, doi:10.5194/acp-9-4115-2009, 2009.

Xia, X., Eck, T. F., Holben, B. N., Philippe, G., and Chen, H.: Analysis of the weekly cycle of aerosol optical depth using AERONET and MODIS data, J. Geophys. Res., 113, D14217, doi:10.1029/2007JD009604, 2008.